ELSEVIER

International Journal of Pharmaceutics 198 (2000) 113–134

international journal of pharmaceutics

www.elsevier.com/locate/ijpharm

Thermodynamic analysis of compact formation; compaction, unloading, and ejection
I. Design and development of a compaction calorimeter and mechanical and thermal energy determinations of powder compaction

Mark T. DeCrosta [a,b,*], Joseph B. Schwartz [b], Rodney J. Wigent [b], Keith Marshall [c]

[a] *SmithKline Beecham Pharmaceuticals, Collegeville, PA 19426, USA*
[b] *Philadelphia College of Pharmacy and Science, Philadelphia, PA 19104, USA*
[c] *Keith Marshall Associates, Brick, NJ 08723, USA*

Received 6 April 1998; received in revised form 3 February 1999; accepted 8 December 1999

Abstract

The aim of this investigation was to determine and evaluate the thermodynamic properties, i.e. heat, work, and internal energy change, of the compaction process by developing a 'Compaction Calorimeter'. Compaction of common excipients and acetaminophen was performed by a double-ended, constant-strain tableting waveform utilizing an instrumented 'Compaction Simulator.' A constant-strain waveform provides a specific quantity of applied compaction work. A calorimeter, built around the dies, used a metal oxide thermistor to measure the temperature of the system. A resolution of 0.0001°C with a sampling time of 5 s was used to monitor the temperature. An aluminum die within a plastic insulating die, in conjunction with fiberglass punches, comprised the calorimeter. Mechanical (work) and thermal (heat) calibrations of the elastic punch deformation were performed. An energy correction method was outlined to account for system heat effects and mechanical work of the punches. Compaction simulator transducers measured upper and lower punch forces and displacements. Measurements of the effective heat capacity of the samples were performed utilizing an electrical resistance heater. Specific heat capacities of the samples were determined by differential scanning calorimetry. The calibration techniques were utilized to determine heat, work, and the change in internal energies of powder compaction. Future publications will address the thermodynamic evaluation of the tablet sub-processes of unloading and ejection.

Keywords: Compaction; Unloading; Ejection; Decompression; Calorimetry; Compaction calorimeter; Compaction work; Compaction heat; Internal energy change; Punch deformation

* Corresponding author.

PII: S0378-5173(99)00466-4

1. Introduction

The objective of this paper is to describe the results of building a compaction calorimeter and its application to determine mechanical and thermal energies of compaction of the test materials. The process to determine the thermodynamics of compact unloading and ejection is also described. Future publications will report these results.

In order to thermodynamically assess tablet formation, the work and heat of the tableting process must be determined. By the use of an instrumented tablet press, or as in this investigation a single tablet 'Compaction Simulator' machine, work was determined from force and displacement measurements. Heat determination was facilitated by adapting a calorimeter to an instrumented tableting machine. This apparatus is termed a 'compaction (compression) calorimeter' (Coffin-Beach, 1982; Wurster and Creekmore, 1986; Rowlings, 1989; Rowlings et al., 1995; Wurster et al., 1995. The calorimeter's function is to insulate the material being compacted in order to measure the change in temperature during tableting. The change in temperature, in conjunction with the heat capacity of the compacted materials, is used to calculate the liberated or absorbed heat from the reaction. Previous investigators have evaluated the mechanical (Higuchi et al., 1953; Nelson et al., 1955; Rankell and Highuchi, 1968; Ragnarsson and Sjogren, 1983; Oates and Mitchell, 1989; Hoblitzell and Rhodes, 1990; Pesonen and Paronen, 1990; Wray, 1992; Oates and Mitchell, 1994) and thermal energies of only the compaction process (Krogerus et al., 1969; Travers and Merriman, 1970; Juslin and Jarvinen, 1971a; Travers et al., 1972; Nurnberg and Hopp, 1981; Coffin-Beach, 1982; Coffin-Beach and Hollenbeck, 1983; Yu et al., 1988; Celik and Maganti, 1994; Rowlings et al., 1995; Wurster et al., 1995). Some authors have evaluated both the mechanical and thermal energies of compaction using a single station hydraulic press (Coffin-Beach, 1982; Coffin-Beach and Hollenbeck, 1983; Rowlings, 1989; Rowlings et al., 1995; Wurster et al., 1995). Due to the limitations of these presses, the authors have not investigated the thermodynamics of the tablet sub-processes of unloading and ejection.

In addition, due to the limitations of single station hydraulic presses working under constant load, stress decay of the powder test materials results. 'True' compaction can not be evaluated. There is additional punch penetration into the compact as the material exhibit stress decay. The present investigation used a compaction simulator which is capable of applying a constant strain waveform.

One of the key functions of compaction studies in pharmaceutical research is to predict compaction behavior and the ability to form a tablet of a powder formulation on a high speed production rotary tablet press. There are numerous procedures for compaction data collection and analysis with their specific applications and limitations. Only recently has someone addressed a standardized procedure for compaction studies (Celik and Okutgen, 1993). Most studies only evaluate the mechanical energy involved in the tablet process and not the thermal consequences. Ideally, a compaction calorimeter should be based on a rotary tablet press, but several limitations exist. The calorimeter's function is to insulate the material being compacted. The rotary tablet press contains the powder inside a 'heat sink' of a stainless steel die and punches. Some investigators have attempted to determine the heat of tablet formation from tablets ejected from eccentric and rotary presses (Hanus and King, 1968; Juslin and Jarvinen, 1971a; Juslin and Krogerus, 1971b; Fuhrer and Parmentier, 1977; Nurnberg and Hopp, 1981; Bechard and Down, 1992; Ketolainen et al., 1993). This does not allow the separate heat determinations of the tablet sub-processes of powder compaction and tablet unloading/ejection. The background heat effects of the press would also make it difficult to differentiate the separate heats.

Instrumented hydraulic presses have been used to compensate for the temperature measurement limitations of eccentric and rotary presses. These presses are capable of making single compactions and are adaptable to thermal measuring devices. These presses utilized thermally insulated punch and die sets which contained the tablet and its corresponding heat inside the die until the change in temperature could be measured (Lammens,

1980a; Coffin-Beach, 1982; Coffin-Beach and Hollenbeck, 1983; Wurster and Creekmore, 1986; Rowlings, 1989; Rowlings et al., 1995; Wurster et al., 1995). By making single compactions, resolution of the heat of compaction from the other thermal processes, which included an equilibrium heat transfer between tablet and press, was possible.

Lammens (1980a), Coffin-Beach (1982), and Coffin-Beach and Hollenbeck (1983) used temperature sensors remote to the powder bed being compacted in conjunction with a die within an insulating die apparatus. In these investigations, the high thermal conductivity of a metal inner die facilitated the transfer of heat to the sensor.

Lammens (1980a) measured the temperature rise after tablet formation, i.e. as a result of both compaction and unloading. Compactions were made in a single punch press that was altered to prevent tablet ejection.

Coffin-Beach (1982) and Coffin-Beach and Hollenbeck (1983) evaluated the compaction process of the tableting cycle with the use of a motorized hydraulic press. A quartz thermometer, immersed in a mercury pool contained between the inner metal die and outer insulating thermoplastic die, measured the temperature rise during compaction. A constant force was applied for ≈ 4 s. The change in temperature, and hence, heat, was measured for the compaction process. Coffin-Beach only evaluated the compaction process and not the subsequent processes of unloading and ejection.

Wurster and Creekmore (1986) monitored temperature with a temperature probe located inside a single component powder sample as it was compacted. The temperature probe was a coiled tungsten wire with its resistance calibrated against temperature. The punch and die assembly was made of polymethyl-methacrylate which was able to withstand the compaction forces and act as an insulator. Compactions were made on a hydraulic laboratory press with dwell times of 40 s under constant force conditions. The temperature rise was measured for the compaction process and corrected for background heat effects.

Wurster et al. (1995) and Rowlings et al. (1995) utilized a modified form of the plexiglass punch and die apparatus of Wurster and Creekmore (1986). A hydraulic press provided a reproducible loading rate and maintained a constant compaction pressure for a 40 s dwell time. The heat of compaction was determined independently by two different temperature probes. Calibration of resistance versus temperature was performed before, during, and after compaction for a tungsten wire temperature probe. The calibration curves were indistinguishable and, therefore, compaction force had a negligible effect on the wire's resistance. The effective heat capacities of the system containing the test material were determined by simultaneously compressing the powder sample and liberating heat from an electrical resistance heater. Corrections were made for the background heat effects of the test materials. Heat capacities of the compacted powders were determined by differential scanning calorimetry. The rank orders of compactional heats for both temperature sensors were the same.

2. Materials and methods

Powders for tableting were chosen to encompass brittle, plastic, and viscoelastic compaction behavior with either good or poor compactibility. These powders include commonly used excipients as well as powders which do not form compacts, i.e. polyethylene, or from capped tablets, i.e. acetaminophen. These materials are: Acetaminophen USP dense powder — Mallinckrodt Specialty Chemicals Company, Raleigh, NC (lot # 5543993B723); Avicel® pH 102 (microcrystalline cellulose) — FMC Corporation, Philadelphia, PA (lot # 2233); Emcompress® (dibasic calcium phosphate dihydrate, USP) — Mendell, Patterson, NY (lot # 7002X); Fast Flo Lactose # 316® — Foremost, Baraboo, WI (lot # 2RL223); low density polyethylene (average molecular weight 35 000) — Aldrich Chemical Company, Milwaukee, WI (lot # 02526LG); Starch 1500 (modified corn starch) — Colorcon, Indianapolis, IN (lot # 201010). Particle sizes of 150–200 microns for all materials, except 212–300 microns for polyethylene, were used in this investigation.

2.1. Compaction calorimeter

The compaction calorimeter (DeCrosta, 1998) is comprised of an aluminum die contained within a Delrin® (acetal resin thermoplastic) die and mandrel-formed fiberglass G-10 flat-faced punches with aluminum tips (Fig. 1). Both the aluminum die and punch tips are made of a durable aluminum alloy which has a high thermal conductivity and a low specific heat (Coffin-Beach, 1982). Delrin® was chosen for its low thermal conductivity to insulate the tableting process. Two aluminum discs, 19.02 mm in diameter and 1.95 mm thick, were epoxied onto the 18.92 mm diameter fiberglass punch tips. A 1 mm diameter bare thermistor probe was glued with a thermally conductive silver epoxy in a 1 mm deep by 1 mm diameter hole drilled in the outside of the aluminum die. The probe was attached to a microprocessor which measures resistance and calculates temperature with high resolution and speed. The resolution of the probe is 0.00001°C using a rating period (time between sampling points) of 100 s and has a <1.6 s temperature response time for the bare thermistor and 42.5 s in-situ. In this investigation, temperature data was monitored and collected every 5 s by the microprocessor with a resolution of 0.0001°C. The temperature was exported to a computer to construct temperature versus time profiles.

2.2. Determination of ΔT of compaction

The change in temperature, ΔT, during compaction was based on Dickinson's graphical extrapolation described by Wadso (Wadso, 1966). The data captured by the microprocessor were analyzed statistically by an Excel® Macro to fit curves to the thermograms and determine the change in temperature during compaction. A linear equation was fit to both the pre- and post-reaction periods and a 5th-order polynomial to the reaction period. The reaction period is the period of temperature rise during compaction or ejection, or the temperature decrease during unloading. An example of an exothermic thermogram is depicted in Fig. 2. A vertical distance, R, is measured between the two extrapolated lines (pre- and post-reaction) at a point near the middle of the reaction period. The vertical distance is then multiplied by 0.63. This distance is then used to locate a vertical intercept with the thermogram originating from the preperiod extrapolated line. The initial temperature, T_i, and the final tempera-

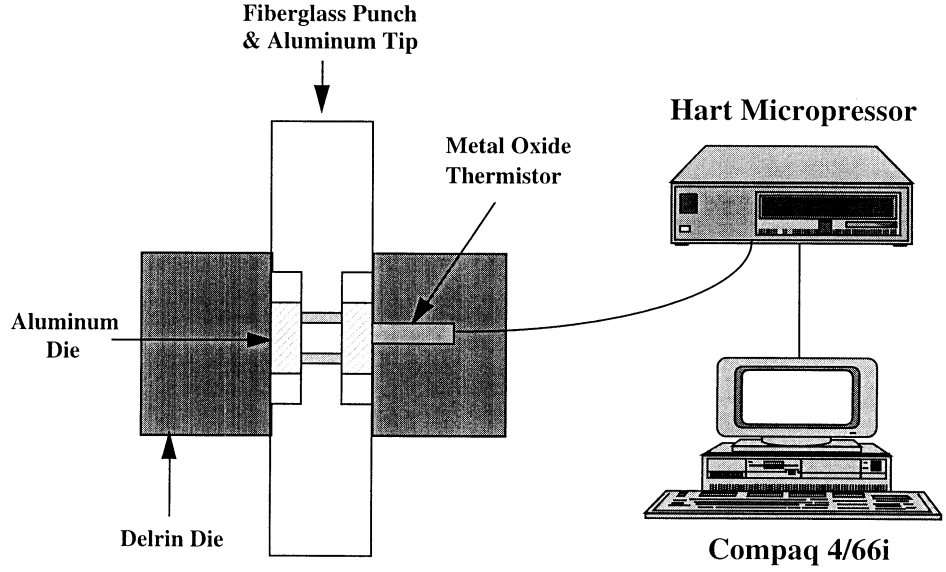

Fig. 1. Compaction calorimeter and temperature data collection apparatus.

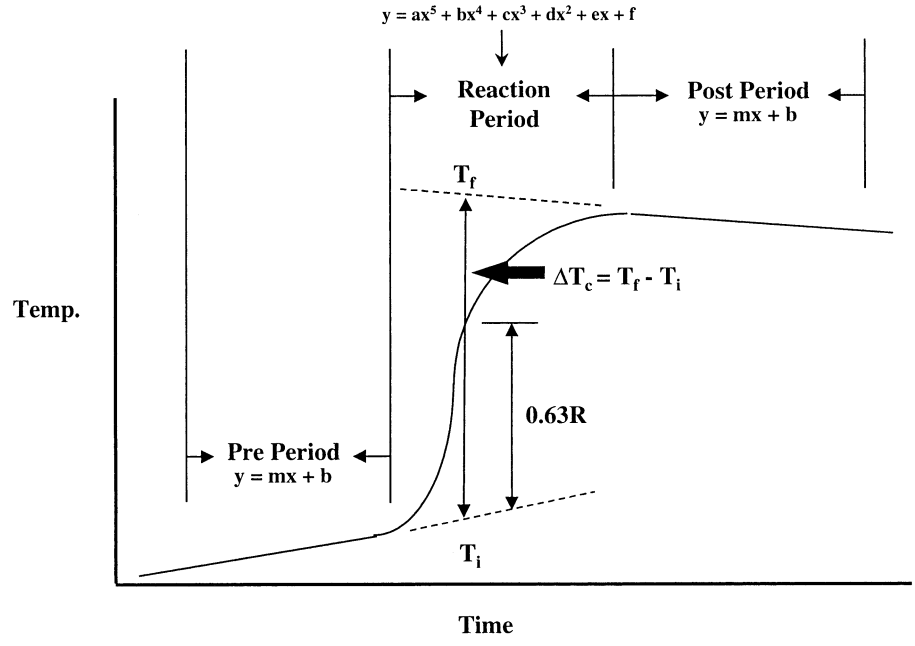

Fig. 2. Schematic of corrected temperature change determination.

ture, T_f, at the intersection points with the extrapolated lines of the pre- and post-periods, are subtracted to determine the corrected temperature rise, ΔT_c. The thermogram in Fig. 2 illustrates the change in temperature for an exothermic reaction, i.e. compaction and ejection. The same technique can be used to determine the temperature change during an endothermic reaction, i.e. unloading.

2.3. Compaction simulator

Compaction of the powder materials was performed by a Compaction Simulator, i.e. an instrumented single-station tablet machine (Mand Testing Machine Ltd. Stourbridge, UK). The components of this machine have been previously described by Celik and Marshall (1989) and Holman and Marshall (1993). Upper and lower punch linear variable differential transducers (LVDTs) with a 10 mm working range and a resolution of 0.01 mm were used to measure punch displacement. Load cells were utilized to measure applied forces up to 50 with 0.01 kN resolution. Compactions of powders were made under constant strain, i.e. constant punch position, for dwell times of 121.65 s. A personal computer, which generates the operating waveform for tableting, relays the information to the machine unit via an electronic link.

The force (load cells) and displacement (LVDT) measurements were relayed to a 16 bit Nicolet 440 digital storage oscilloscope (Nicolet Instruments Corp., Madison, WI). The oscilliscope can capture 16 K of data per each of four channels. Data was stored to each of the four channels, two channels for LVDT data and two channels for load cell data. The Nicolet was configured to capture 3000 data points at 0.050 s/pt during compaction and unloading, and 3000 points at 0.001 s/pt during ejection. The voltage scale for the compaction and unloading phase for channels 1 and 3 (load cells) was set at 12 and 30 V for channels 2 and 4 (LVDT's). The voltage scale for ejection was set at 1.2 V for channels 1 and 3, and 30 V for channels 2 and 4. During ejection smaller forces, compared to compaction, are needed to remove the compact from the die. As a result, the voltage sensitivity was increased for ejection.

Compaction and unloading of the powders were performed using a 'step like' double-ended

punch waveform with 0.03 s increments (Fig. 3). The upper punch displacement was 8 mm and the lower punch displacement was 5 mm. The punch displacement speed for both compaction and unloading was 6.7 mm/s for the upper punch and 4.2 mm/s for the lower punch. The speed of ejection was 200 mm/s. The compaction of the powder occurred in 1.2 s with a subsequent period of 121.65 s (122.85 − 1.2 s) at constant strain. The compaction simulator master database program 'CONSIM' program (Celik and Marshall, 1989) (originally written by Abacus Industries Ltd, Stourbridge, UK) was altered (by Greaves–Guant Control Systems, Kinver, UK) to pause the simulator before ejection. The altered program enabled the operator to press any key on the keyboard, after the 122.85 s constant strain period, to initiate the ejection process. This pause accounted for the ≈ 90 s lag time needed to measure the total change in temperature of the compacted powder as a result of unloading. Compaction of the powder material was not initiated until a change in temperature of < 0.001°C was observed for at least six consecutive rating periods, i.e. ≈ 30 s.

2.4. Specific and effective heat capacities

The specific heat capacities (constant pressure) of the compacted materials were determined by Seiko Instruments' Inc. SSC5200 Thermal Analysis System Optional Software Series DSCSUB and DSCCP using the Seiko Differential Scanning Calorimetry (DSC) Model DSC120 (Seiko Instruments Inc., Horsham, PA). Nitrogen, at 40 ml/min, was used as a purge gas and ice was used to cool the DSC cell to 0°C before the start of each run. Heat capacities were determined between 0 and 60°C at a heating rate of 1°C/min. Computation of specific heat capacities were performed using synthetic sapphire (Al_2O_3) as the reference. The weight of the compacted materials were ≈ 4–5 mg.

The effective heat capacity of the punch and die assembly, with and without the compacted materials, was obtained by liberating a quantity of heat, as electrical work, using a resistance heater and measuring the increase in temperature. Materials were compacted at a force of 30 kN. An alternate lower punch was used as a replacement during effective heat capacity measurements. This alternate punch contained a resistance heater and was used in Coffin-Beach's compaction calorimetry work (Coffin-Beach 1982; Coffin-Beach and Hollenbeck, 1983). A nichrome wire was wrapped around a core of the same fiberglass material, G-10, used in the compression punches (Coffin-Beach 1982). The wire wrapped fiberglass was placed on the tip of the punch with the wire leads inserted through holes cut through to the punch end. The nichrome heater was placed in parallel with a DC power source (HP E3610A Lab Bench Power Supply-Hewlett Packard, Loveland, CO) and a double-pole, double pull switch connected to a timer (Model # 636 type 10072 elapsed timer-Newark Electronics, Newark, NJ) with 0.1 s resolution. When the switch was activated, voltage from the power source flowed through the resistance heater and simultaneously started the timer. The amount of heat generated by electrical work is determined from the following:

$$W_{\text{elect}} = V \cdot I \cdot t = (V^2/R) \cdot t; \quad (1)$$

where V is the voltage; I is the current; R is the resistance of nichrome wire; and t is the time of applied voltage. The DC power source was set on constant current at a voltage of 2.00 V and the resistance heater was excited for a period of 10.0 s. In order to more accurately measure the applied voltage, a Fluke multimeter, with a resolution of 0.00001 V, was connected to the power source.

True density, bulk density, moisture content, and mass of the materials are presented in Table 1. True densities of the test materials were determined by Helium pycnometry (Accupyc Model # 1330-Micromeritics, Norcross, GA) with an equilibration rate of 0.005 psig/min. True densities of the materials were needed to determine the mass of each powder which would be equivalent to a theoretical thickness of 3.81 mm and a true volume of 1.0774 cm^3 at zero porosity when compacted. True densities were measured for the compacts and represented no significant difference compared to their respective powders. Bulk densities were determined by weighing the mass corresponding to a 50 ml vol. in a volumetric cylinder.

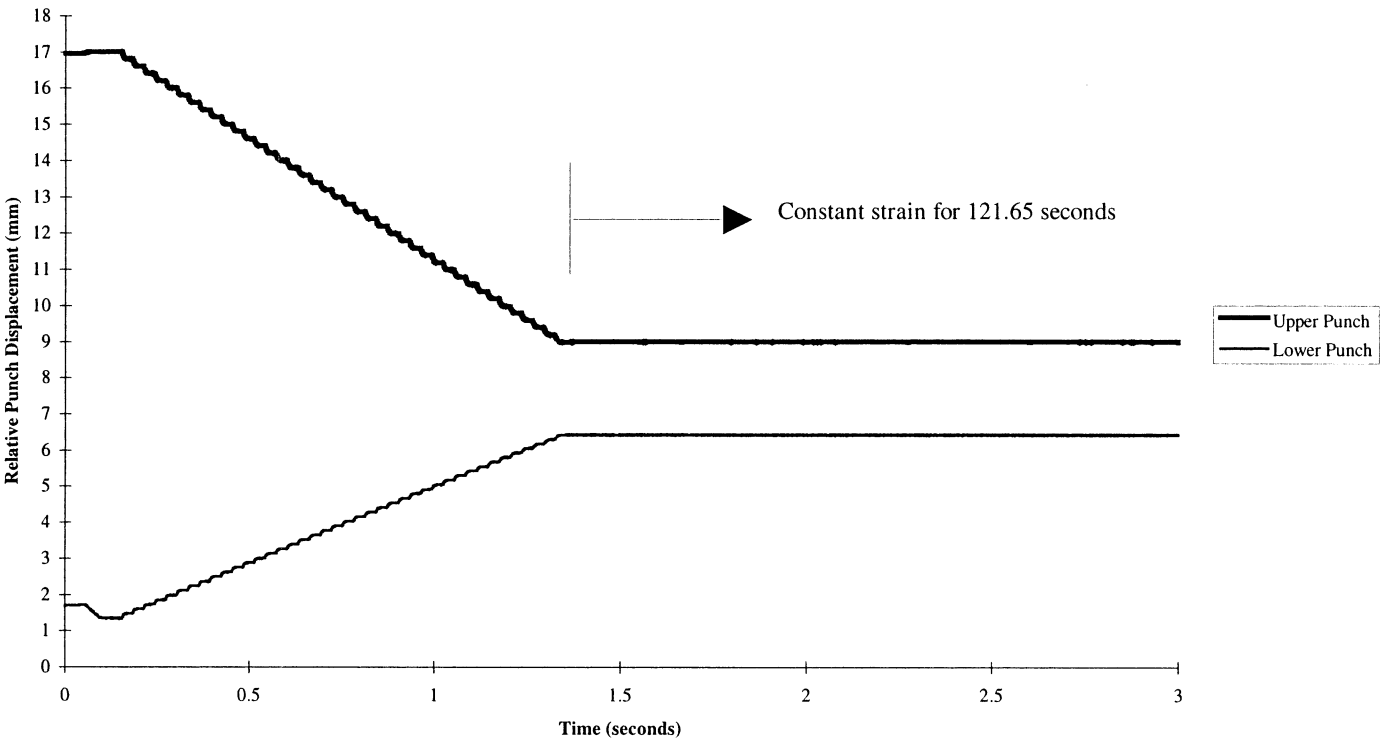

Fig. 3. Double-ended compaction profile.

Moisture contents of the materials, by determining their weight loss on drying, were performed gravimetrically using a Motorola Computrac MAX50 (Motorola Inc., Mansfield, MA).

3. Results and discussion

3.1. Mechanical calibration

In order to determine the work and heat of powder compaction and tablet unloading and ejection, the effects of the empty punch and die system need to be determined. As force was applied to the punches they compress, producing elastic work, and also liberating heat due to the compression. Both the mechanical and thermal effects of the elasticity of the fiberglass punches, under load, were accounted for by two calibration techniques. The mechanical energy, i.e. work, of the elastic deformation of the punches, was derived from a calibration curve plotting punch displacement versus applied force. The calibration experiment consisted of placing the punches tip to tip at 0.00 kN after which the load was increased continuously to ≈ 45 kN and then decreased back to 0.00 kN. Both punch displacement and applied force for both punches were recorded by the Nicolet 440 oscilloscope at a rate of 0.02 s/pt for 2000 pts. Both the up and down curves of punch displacement versus applied force plot were superimposable, indicating only an elastic compression of the punches (Fig. 4). If plastic compaction was also present, the curves would be significantly offset from each other. A fourth order polynomial was fitted to the data with a resulting R^2 value of 0.9989. This calibration experiment was only indicative of the relative positions of the LVDTs, since the punches are face to face at the start of the experiment. The LVDTs were attached to the barrels of both the lower and upper punches. As force is applied to the punches and they begin to compress, the relative positions of the LVDTs indicate that they are closer than at the start. This observed displacement by the LVDTs needs to be accounted for, i.e. by subtraction, from the displacements observed for experiments compressing the powder test materials. The work resulting from the elastic deformation of the punches was calculated from the area under the punch displacement versus force curve. The work versus applied force plot for 'elastic deformation' of the punches is shown in Fig. 5. This work is used to correct the observed work during compaction, unloading, and ejection to differentiate the work attributable only to the compact to that of the punches.

In order to determine the work due to punch friction against the wall of the aluminum die, a 'blank' compaction run was made with the double-ended punch waveform used to compress the powdered materials. The observed forces during the blank run were < 0.10 kN. The resulting

Table 1
Bulk density, true density, moisture content, and mass of powder materials

Material	Approximate bulk density[a] (g/cm^3)	True density[b] (g/cm^3)	Moisture content[c] (%)	Mass of material compacted (g)
Acetaminophen	0.642 (0.007)	1.2938 (0.0001)	0.12 (0.01)	1.6886 ± 0.0005
Avicel® pH 102	0.312 (0.012)	1.5672 (0.0033)	3.07 (0.15)	1.3940 ± 0.0005
Emcompress®	0.858 (0.011)	2.3083 (0.0009)	0.75 (0.01)	2.487 ± 0.0005
Fast Flo Lactose # 316	0.563 (0.011)	1.5423 (0.0023)	0.75 (0.05)	1.6220 ± 0.0005
Starch 1500	0.670 (0.008)	1.5002 (0.0001)	8.09 (0.16)	1.6092 ± 0.0005

[a] Sample size $n = 4$, standard deviations are in parentheses.
[b] Sample size $n = 6$, standard deviations are in parentheses.
[c] Sample size $n = 2$, standard deviations are in parentheses.

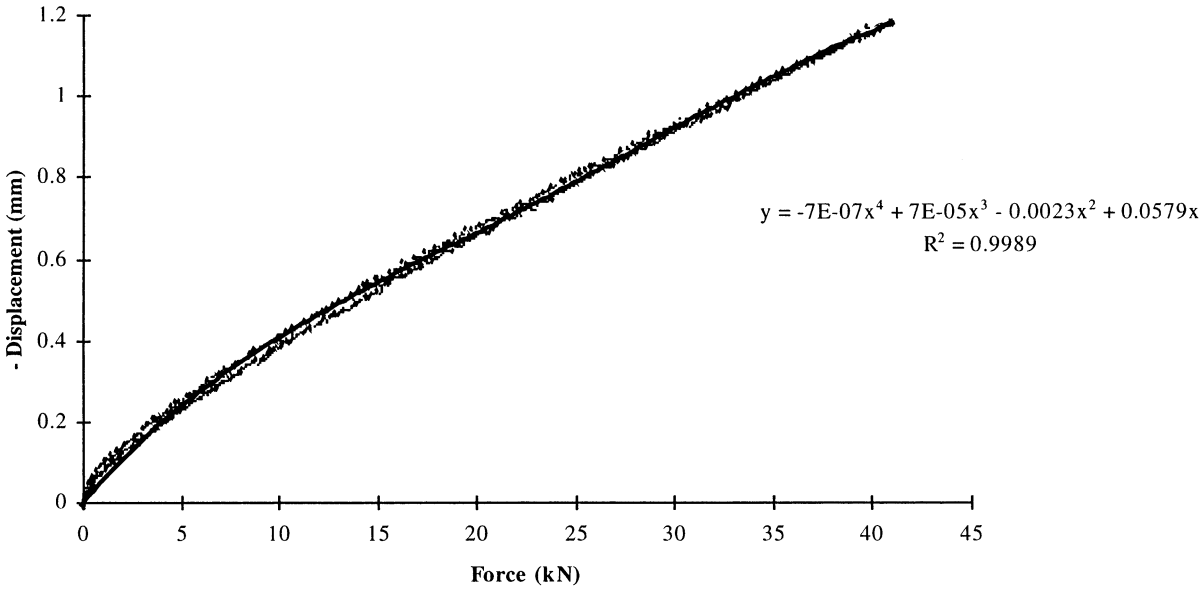

Fig. 4. Negative distance between punches (determined by LVDTs) versus applied punch force.

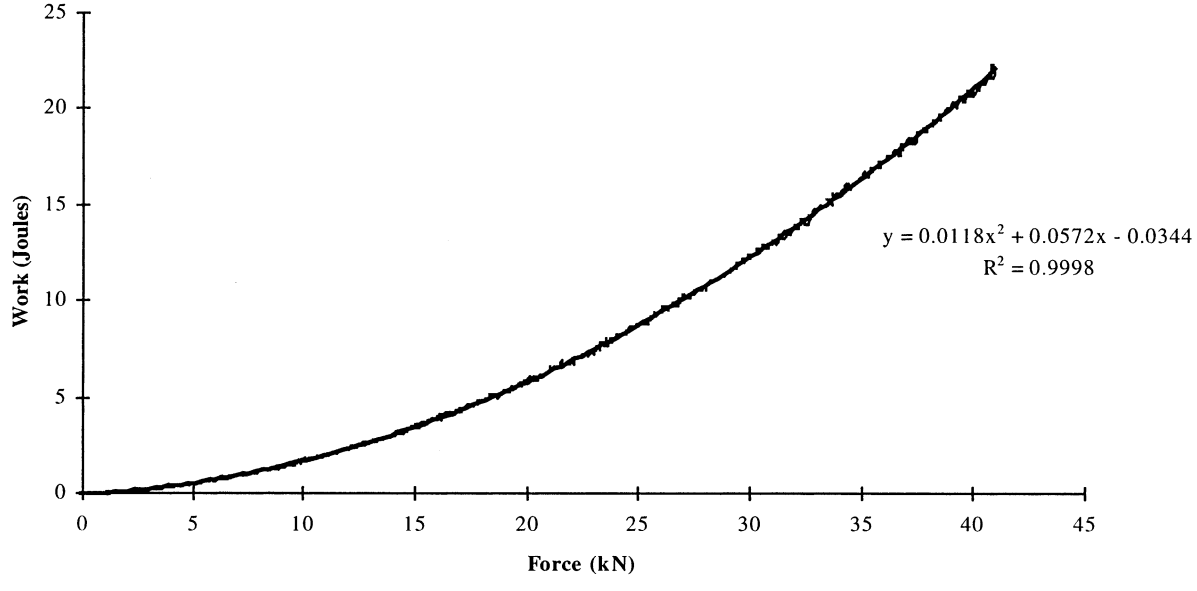

Fig. 5. Elastic punch deformation work versus applied punch force.

values of frictional work were determined to be negligible. A 2% stearic acid solution, as a lubricant, was applied to the aluminum die with acotton swab before the blank compactions as well as compactions of the test materials.

3.2. Thermal calibration

The thermal effects of the compression and decompression of the fiberglass punches from 'blank compaction' runs, i.e. without test materi-

als, were determined from a temperature versus applied load calibration plot. The thermal calibration experiments consisted of placing the punches tip to tip, applying instantaneously an applied force from 0.00 to 45 kN. Temperature was monitored by the thermistor before, during, and after applying a specific force to the punches. After a difference in temperature of < 0.001°C was observed for consecutive ratings, temperature data collection was initiated. As a force was applied to the punches, a rise in temperature was observed. After the peak temperature was observed for the blank compression, the temperature was monitored for at least 90 s, after which the applied force was removed. The resulting decrease in temperature was observed for ≈ 90 s after the applied force was removed. The temperature increase during compression of the punches was found to be the same as the decrease during unloading confirming that only elastic deformation of the punches occurred. Therefore, the temperature versus compression force profile can be used to calculate the temperature decrease during unloading simply by using the negative temperature change during compression at the corresponding applied force. A typical temperature profile for compression and unloading of the fiberglass punches, applying a 41.54 kN, force is shown in Fig. 6. The resulting thermal calibration curve for the elastic deformation of the fiberglass punches at several applied forces is displayed in Fig. 7. The determined regression equation is:

$$Y(\text{temperature change}) = 0.001937 \times (\text{applied force}) - 0.000327 \quad (2)$$

The slope of the linear regression line was statistically significant (P value < 0.05, i.e. $1.11\text{E}-10$) and the Y-intercept was not statistically significant (P value > 0.05, i.e. 0.56). The observed temperature change during compaction and unloading of a powder, as well as ejection of the resulting tablet, was corrected using the values from this curve. For compaction of a powder, the thermal calibration temperature, corresponding to the applied force during compaction, is subtracted from the observed increase in temperature during powder compaction. The corresponding temperature is also subtracted from the temperature increase during tablet ejection. The calibration temperature is added for the temperature decrease during tablet unloading. The net corrected temperatures for the tablet sub-processes are then used to calculate the heats of compaction, unloading, and ejection (DeCrosta, 1998).

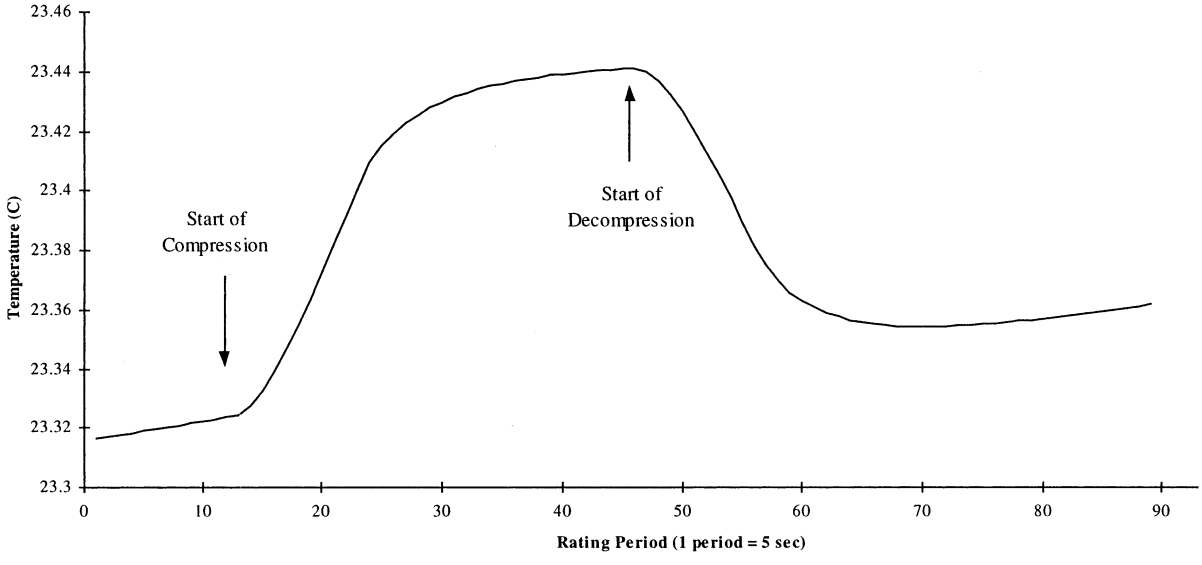

Fig. 6. Thermal calibration of elastic punch deformation — compression at 41.54 kN punches tip to tip.

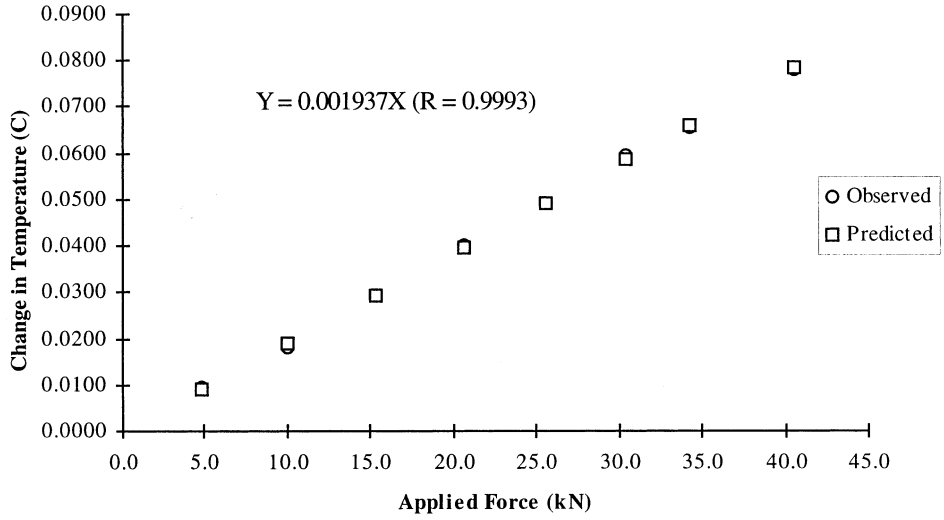

Fig. 7. Thermal calibration curve of elastic deformation of punches.

3.3. Determination of work, heat, and internal energy change

By determining the temperature rise during punch compression, the corresponding heats for compaction, unloading, and ejection can be calculated. Some investigators have determined the heat of compact formation (Coffin-Beach, 1982; Coffin-Beach and Hollenbeck, 1983; Rowlings et al., 1995; Wurster et al., 1995). By determining the temperature changes during compaction and determining both the heat capacities of the test materials and compaction apparatus, the heat of compaction (Q_c) can be calculated. In this investigation, the heats of tablet unloading ($Q_{unloading}$), and ejection (Q_e) were also determined due to the application of a constant strain punch profile obtained only with a Compaction Simulator. System heat effects, such as punch deformation and friction between the punches and die, are accounted for by correcting the measured heats.

The first law of thermodynamics is defined as;

$$\Delta E = Q + W; \tag{3}$$

where ΔE is the change in internal energy of the system as the result of a process, Q is the heat of the system, and W is the work of the system. The conventions of the signs of Q and W are set from the system's viewpoint. When heat flows into the system, Q is positive and when heat flows out of the system Q is negative. Work done on the system is positive and work done by the system is negative.

For a powder compact, i.e. tablet, formed between the punches contained inside the calorimeter, the compact/tablet is considered the system, and the calorimeter, punches, etc. are considered the surroundings. Work done on or by the system is calculated from:

$$W = -PdV = -P(V_{final} - V_{initial}) \text{ where;} \tag{4}$$

P is the pressure applied on or by the system and dV is the change in volume of the compacted material. The volume (V) of the tablet is defined as $V = \pi r^2 h$, where r is the radius of the tablet and h is the height (thickness) of the tablet. The radius of the tablet contained inside the die is assumed not to change, therefore;

$$W = -P\pi r^2(h_{final} - h_{initial}). \tag{5}$$

Heat absorbed or liberated by the system is calculated from:

$$Q = m \cdot C_p \cdot \Delta T = m \cdot C_p \cdot (T_{final} - T_{initial}) \text{ where;} \tag{6}$$

$T_{initial}$ and T_{final} are the temperatures before and after, respectively, of compaction, unloading, and ejection;

$T_{initial}$ is the temperature before compaction, unloading, or ejection;
m is the mass of the compressed sample; and
C_p is the specific heat capacity at constant pressure.

From the first law of thermodynamics, the heat released or absorbed by the system must be absorbed or released by the surroundings, hence;

$$Q_{system} + Q_{surroundings} = 0; \quad (7)$$

$$Q_{system} = -Q_{surroundings}; \quad (8)$$

Defining;

$$Q_{system} = Q_{sample} + Q_{friction}; \quad (9)$$

and;

$$Q_{surroundings} = Q_{calorimeter} + Q_{punches}; \quad (10)$$

then;

$$Q_{calorimeter} + Q_{punches} + Q_{sample} + Q_{friction} = 0 \quad (11)$$

The heat liberated during compaction of the powder or ejection of the tablet must be absorbed by the surroundings, i.e. punches and calorimeter.

The thermal affects of the punches from applied forces during tableting are determined from blank compaction runs. The punch tips and aluminum die were lubricated with a 2% lubricant (stearic acid)/acetone solution applied by a cotton swab. The stearic acid reduced friction of the punch tips against the die wall that produced negligible heats during 'blank' compaction runs. Therefore, $Q_{friction} = 0$ for blank compaction runs. In addition, since no material is being compacted, $Q_{sample} = 0$. Then;

$$Q_{punches} = -(Q_{calorimeter}) = -[Q_{calorimeter(blank)}] \quad (12)$$

For compaction and ejection, where $T_{final} > T_{initial}$, $Q_{punches}$ will be negative as calculated from the positive $Q_{calorimeter(blank)}$. Conversely, for unloading, where $T_{final} < T_{initial}$, $Q_{punches}$ will be positive as determined from the negative $Q_{calorimeter(blank)}$. The values of $Q_{punches}$ will be used in Eq. (12) when determining the heats of compaction, unloading, and ejection of the compacts.

The majority of investigators have determined only the heat of compact. The adaptation of a compaction simulator to produce compacts enables the separation of the tablet sub-processes of compaction, unloading, and ejection. By monitoring temperatures during these process their respect heats can be determined. The determinations of these heats, compaction (Q_c), unloading ($Q_{unloading}$), and ejection (Q_e), are each calculated from the equation below:

$$Q_c \text{ or } Q_{unloading} \text{ or } Q_e = Q_{sample} \quad (13)$$

$$Q_c \text{ or } Q_{unloading} \text{ or } Q_e = -Q_{calorimeter} - Q_{punches} \quad (14)$$

$$Q_c \text{ or } Q_{unloading} \text{ or } Q_e = -Q_{calorimeter} + Q_{calorimeter(blank)} \quad (15)$$

For the compaction of a powder in the compaction calorimeter apparatus, without correcting for punch and calorimeter thermal effects, the heat measured by the calorimeter, i.e. that measured by the thermistor contained within the calorimeter, is calculated by:

$$-Q_{calorimeter} = Q_{punches} + Q_{sample} \quad (16)$$

$$-Q_{calorimeter} = \Delta T \cdot C_{p,effective} \quad (17)$$

where ΔT is the temperature change during the process, and $C_{p,effective}$ is the heat capacity of the punch and die apparatus containing the test material. The heat capacity equation which corrects for thermal effects of the calorimeter is:

$$C_{p,calorimeter} = C_{p,effective} - C_{p,compound}; \quad (18)$$

$$C_{p,calorimeter} = C_{p,effective} - (C_{pDSC} \times m_{tablet}) = J/°C; \quad (19)$$

where $C_{p,calorimeter}$ is the effective heat capacity (J/°C) contribution of the punch and die to the material contained inside; C_{pDSC} is the specific heat capacity of the test material determined by differential scanning calorimetry; and m_{tablet} is the mass of the tablet. When no material is contained inside the calorimeter, i.e just air, then $C_{p,calorimeter}$, i.e. $C_{p,calorimeter(blank)}$, is equal to $C_{p,effective}$. The calculated heat (Eq. (21)) is the thermal effects of elastic deformation of the punches (Eq. (12)) due to the applied force. By determining the heat capacity of the calorimeter, the heat during the process as measured by the

calorimeter containing the powder and of the empty calorimeter, i.e. without powder, can be calculated from:

$$Q_{\text{calorimeter}} = \Delta T \cdot C_{\text{p,calorimeter}} \quad (20)$$

$$Q_{\text{calorimeter(blank)}} = \Delta T_{\text{blank}} . C_{\text{p,calorimeter(blank)}} \quad (21)$$

where the temperature change in the empty calorimeter is ΔT_{blank}.

To provide comparative analysis, the heats can be calculated on a gram basis by dividing the heat (Q) by the mass of the tablet (m), i.e. Q/m. The heat capacities for each of the compacted materials varied slightly between 15 and 45°C and therefore, the variation within this range was determined to be negligible. Since the compaction process may only produce a theoretical temperature rise of 5–10°C, as Rowlings et al. (1995) observed with their in sample temperature sensor, the heat capacity variation becomes negligible. The heat capacities, at 30°C, for the material compacts are displayed in Table 2. All heat calculations were based on the heat capacities of the material compacts at 30°C as was performed by Wurster et al. (1995)).

Effective heat capacities (system + tablet) of the compressed tablets are shown in Table 2. These heat capacities were used in Eq. (6) to determine the heat capacity of the system and subsequently, the heat of the system from equation Eq. (7).

Table 2
Effective and specific heat capacities of compacts

Material	Effective heat capacity (C_p) J/C	DSC specific heats J/gC
Acetaminophen (APAP)	139.7 ± 1.9	1.653
Avicel® pH 102 (AV)	136.3 ± 1.6	1.345
Emcompress® (EMC)	139.2 ± 1.7	0.950
Lactose (LACT)	139.5 ± 1.8	1.004
Starch 1500 (STR)	142.0 ± 1.8	1.669
Polyethylene (PE)	140.1 ± 2.3	[a]

[a] Did not form compact, C_p of powder.

3.4. Work of compaction

Increased tensile strength (Krycer et al., 1982; Leuenberger, 1982; Jetzer et al., 1983; Esezobo and Pilpel, 1987; Celik, 1992) has been shown to be a function of increased compaction forces. As compaction forces increase, brittle materials fracture or plastic materials flow. As a result, additional particle surface area becomes available for particle contact. This increase in particle surface contact promotes a possible increase in bonding. Coffin-Beach (1982) and Coffin-Beach and Hollenbeck (1983) reported work and heat as a function of applied compaction force from 5 to 30 kN. Coffin-Beach also reported that a reduction in surface area upon compaction was responsible for yielding negative change in internal energies upon compaction of powdered materials. The availability of particle surface area for particle contacts, and, therefore, bonding during compaction, can be measured by determining the porosity level of the compact. Celik and Marshall (1989) were the first to report work and force as a function of porosity. Porosity is the measure of the total intra- and interparticulate voids of a compact. Porosity has an indirect correlation with the quantity of particle surface area for contact. As porosity is reduced, more surface of particles come into contact for the possibility of bonding. Percent porosity (%E) is calculated form the following equation:

$$\%E = 100[1 - (V_t/V_c)] = 100[1 - (H_t/H_c)] \quad (22)$$

where V_t is the volume of the compact at 0% porosity, V_c is the volume of the compact under pressure, H_c is the thickness of the compact under pressure, and H_t is the thickness of the material at 0% porosity. In the present research, work, heat, and internal energy change, will be reported against percent solids as well as maximum compaction force. Percent solids (% Solids) is the quantity of material, excluding voids, i.e. air, contained within a compact. Percent solids of a compact is calculated by subtracting %E from 100: at 100% solids, no voids are present, and, hence, %E equals 0:

$$\%\ \text{Solids} = 100 - \%E \quad (23)$$

The present investigation utilized a constant strain (punch position) waveform for tableting where previous investigations (Coffin-Beach, 1982; Coffin-Beach and Hollenbeck, 1983; Celik and Marshall, 1989; Oates and Mitchell, 1989; Rowlings et al., 1995; Wurster et al., 1995) have used a constant stress (force) profile. A constant strain waveform produces a specific punch displacement during compaction. The force necessary to move the punches the desired distance is a function of the deformation mechanism of the material being compressed. This force is not known until after the compaction event.

Materials held under constant stress conditions may yield stress decay, hence, additional punch movement, and therefore additional compaction work. This additional work is inherent in Coffin-Beach's and Rowlings' work where compaction pressures were held for 4 and 40 s, respectively. Plastic materials will flow under certain forces and, therefore, yield additional punch movement/work under constant stress conditions. Brittle materials allow additional work as a result of additional particle fracture and consolidation.

Work, for a tablet press system, is mechanical energy that is derived from force and displacement measurements (Higuchi et al., 1953, 1954; Nelson et al., 1955; Rankell and Highuchi, 1968; Ragnarsson and Sjogren, 1983, 1985; Oates and Mitchell, 1989; Hoblitzell and Rhodes, 1990; Pesonen and Paronen, 1990; Dwivedi et al., 1992; Wray, 1992; Ketolainen et al., 1993; Oates and Mitchell, 1994). Simply, an applied force, F, over a distance, dX, provides the information to determine work:

$$W = \int F dX \tag{24}$$

In order to derive the total work of compaction (TWC) (Celik and Marshall, 1989) several parameters need to be measured.

$$\mathrm{TWC} = \left(\int_{X=0}^{X\,\mathrm{max(up)}} F_{\mathrm{up}} dX_{\mathrm{up}} \right) + \left(\int_{X=0}^{X\,\mathrm{max(lp)}} F_{\mathrm{lp}} dX_{\mathrm{lp}} \right) \tag{25}$$

where F_{up} and F_{lp} are the forces of the upper and lower punch determined from load cell measurements, X_{up} and X_{lp} are the contributions of the upper and lower punches, respectively, to the decrease in the distance between them as measured by the LVDTs; $X = 0$ is the distance between the punches where pressure is initially observed and $X_{\mathrm{max(up)}}$ and $X_{\mathrm{max(lp)}}$ is the distance observed at maximum pressure. The total work of compaction for each punch includes frictional work, and work due to elastic deformation of the punches under pressure. The same type of equation as Eq. (24) above can be used to determine work of unloading (Dwivedi et al., 1992; Ketolainen et al., 1993), work of ejection (Ketolainen et al., 1993), and work of friction (Jarvinen and Juslin, 1974; Lammens et al., 1980b, 1981; Ragnarsson and Sjogren, 1983; Ketolainen et al., 1993). 'Blank' compactions, i.e. without powder test materials in the system, were performed. Both the punch tips and die were lubricated with a 2% stearic acid/acetone solution prior to each blank compaction. Values for both frictional work and frictional heat were determined to be negligible.

Compaction work was found to increase more for the plastic materials (Avicel® and Starch 1500) than for the brittle materials (Emcompress® and lactose) as seen in Fig. 8 (compaction work vs. maximum compaction force). For brittle materials, as compaction forces increase, particles fracture with a result of increased packing and consolidation of the smaller particles. The increased packing/consolidation of brittle materials yields less additional work than plastic materials as compaction force increases. This can be seen from the larger slopes of Avicel® and Starch curves in Fig. 8 compared to the brittle materials of lactose and Emcompress®. Acetaminophen, which is elastic in nature, has a very low slope. The elasticity of this material does not allow significant punch penetration compared to the other materials.

In addition to plotting compaction work as a function of maximum compaction force, this investigation used a novel reporting of data, i.e. compaction work versus percent solids content (Fig. 9). Typical commercial tablets contain 85–95% solids content, i.e. 5–15% porosity. In Fig. 9,

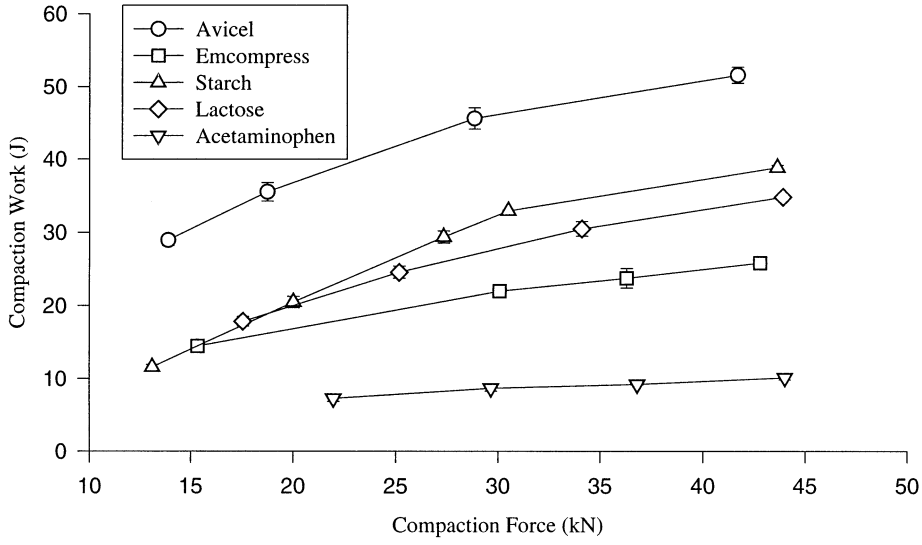

Fig. 8. Compaction work versus maximum compaction force (all points displayed are sample means of $n = 3$ with 2 s error bars).

the rank order of compaction work at 75% solids content of the compacted materials were: Avicel® > Emcompress® > lactose > starch > acetaminophen. Avicel® displays a larger compaction work (30 J) than the brittle materials of lactose (20 J) and Emcompress® (23 J). Avicel®, which flows plastically under applied load, allows greater compression, and hence greater ΔX and therefore, greater work, i.e. $W = F\Delta X$. However, starch, another plastically deforming material, displays a compaction work value of ≈ 13 J. This value is less than both Emcompress® and lactose which may be due to a smaller yield force required for plastic flow. For APAP, forces of only 8–10 kN, produced compacts of 85–88% solids. At 75% solids, APAP had forces appreciably lower than the other materials due to its ease of compression (reduction in volume).

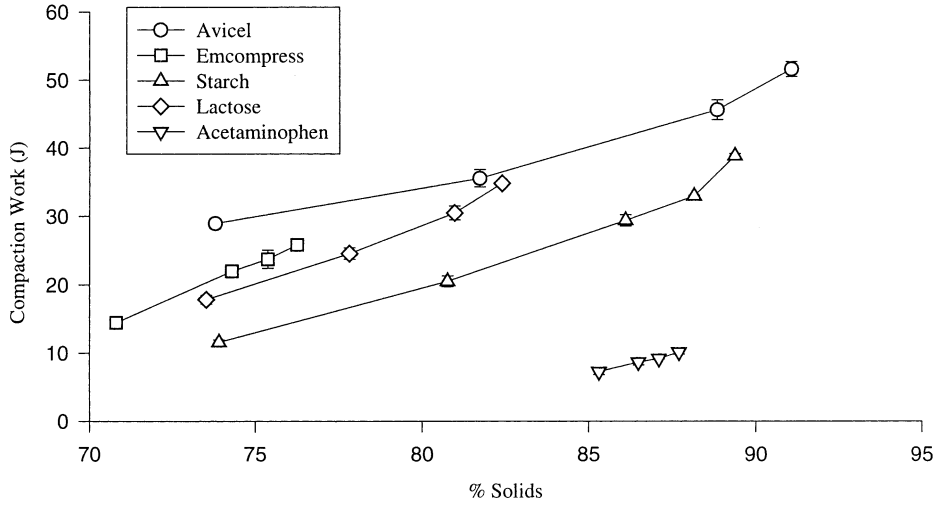

Fig. 9. Compaction work versus % solids content of compact under load (all points displayed are sample means of $n = 3$ with 2 s error bars).

If Emcompress® and lactose curves (Fig. 9) are projected to above 85% solids, these brittle materials appear to show larger work values than the plastic materials of Avicel® and starch. This indicates that larger forces would be needed to fracture particles and allow the resulting smaller particles to occupy additional void space. In addition, larger forces may also be necessary to overcome mechanical interlocking of the particles at high percent solids. The plastic materials yield larger increases in percent solids with increased compaction work than the brittle materials. This is due to the materials flowing plastically and filling void spaces more readily. Acetaminophen requires smaller forces to obtain 85% solids than both the plastic and brittle materials indicating its ease of compression, i.e. volume reduction.

Applied forces over the 122.2 s period of constant strain were monitored by the load cells. Table 3 lists the maximum compaction force and force at unloading initiation for the different compacts. The difference between these forces is the stress decay of the compacted material during the constant strain period. As one can see, stress decay is greater for the plastic materials, Avicel® and starch, than for the brittle materials, Emcompress® and lactose, and APAP, an elastic material. Starch appears to have the largest decay which is indicative of its greater plastic behavior than Avicel®. Lactose, which is partially plastic, displays a slightly larger stress decay than the purely brittle material of Emcompress®. All the materials displayed an approximately constant stress decay over their tested percent solids content except starch.

3.5. Heat of compaction

The relationship of compaction heat, which is an indication of bonding, for the materials can be seen in Figs. 10 and 11. Compaction heat is the result of the bonds formed from the applied energy, i.e. compaction work. Rowlings (1989), Rowlings et al. (1995), Coffin-Beach (1982) and

Table 3
Maximum compaction and unloading forces, and stress decay forces (sample size $n = 3$, standard deviations in parentheses)

Material	Solids content (%)	Maximum compaction force (kN)	Force at unloading initiation (kN)	Stress decay (kN)
APAP	87.7	44.0 (0.1)	40.7 (0.2)	3.3 (0.2)
	87.1	36.8 (0.3)	33.2 (0.0)	3.6 (0.3)
	86.5	29.7 (1.1)	26.4 (0.9)	3.3 (0.2)
	85.3	22.0 (0.4)	18.1 (1.2)	3.9 (0.3)
Avicel® pH102	91.1	41.7 (0.3)	36.4 (0.2)	5.3 (0.1)
	88.8	28.9 (0.4)	22.5 (0.3)	6.4 (0.1)
	81.7	18.7 (0.3)	12.5 (0.5)	6.2 (0.2)
	73.8	13.9 (0.3)	8.5 (0.3)	5.4 (0.1)
Emcompress®	76.3	42.8 (0.7)	39.7 (1.2)	3.1 (0.5)
	75.3	36.3 (0.8)	32.3 (1.5)	4.0 (0.7)
	74.3	30.1 (0.7)	27.0 (0.7)	3.1 (0.2)
	70.8	15.3 (0.1)	12.3 (0.7)	3.0 (0.6)
Lactose	82.4	43.9 (0.1)	39.7 (0.3)	4.2 (0.1)
	81.0	34.1 (1.5)	29.2 (1.7)	4.9 (0.2)
	77.8	25.2 (0.8)	20.3 (1.5)	4.9 (0.9)
	73.5	17.6 (0.8)	12.3 (1.5)	5.3 (0.8)
Starch 1500	89.4	43.6 (0.3)	37.0 (0.4)	6.6 (0.2)
	88.2	30.5 (0.3)	20.4 (0.8)	10.1 (1.0)
	86.1	27.3 (0.6)	18.2 (1.0)	9.1 (0.4)
	80.8	20.0 (0.6)	10.8 (0.6)	9.2 (0.7)
	73.9	13.1 (0.2)	6.10 (0.5)	7.0 (0.7)

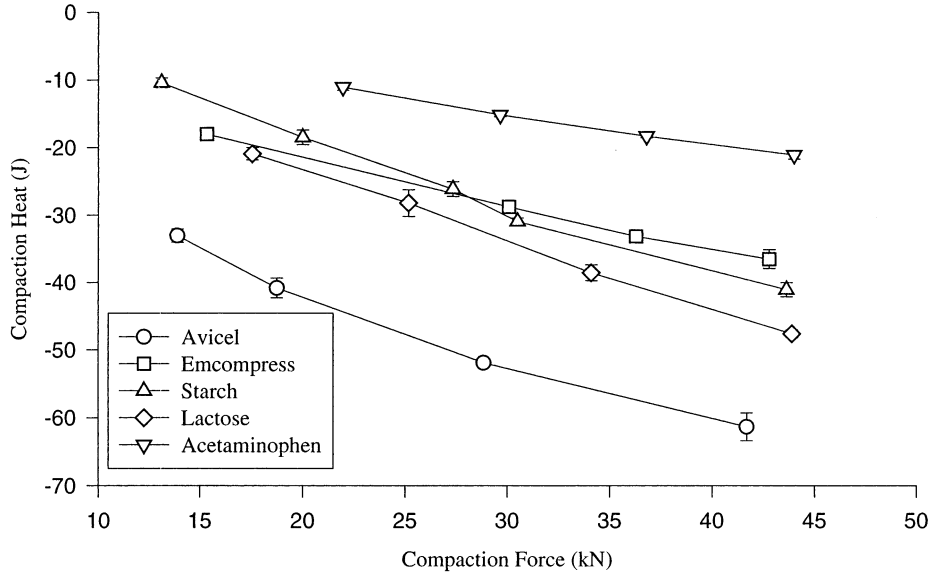

Fig. 10. Compaction heat versus maximum compaction force (all points displayed are sample means of $n = 3$ with 2 s error bars).

Coffin-Beach and Hollenbeck (1983) both showed that compaction is an exothermic process due to bonding. The compaction heat rank order of the materials by both investigators was Avicel® > lactose > starch. This was also seen in this investigation as displayed in Fig. 3 (compaction heat vs. maximum compaction force). Authors (Coffin-Beach, 1982; Coffin-Beach and Hollenbeck, 1983; Hiestand, 1991; Bechard and Down, 1992; Rowlings et al., 1995) have only reported the thermo-

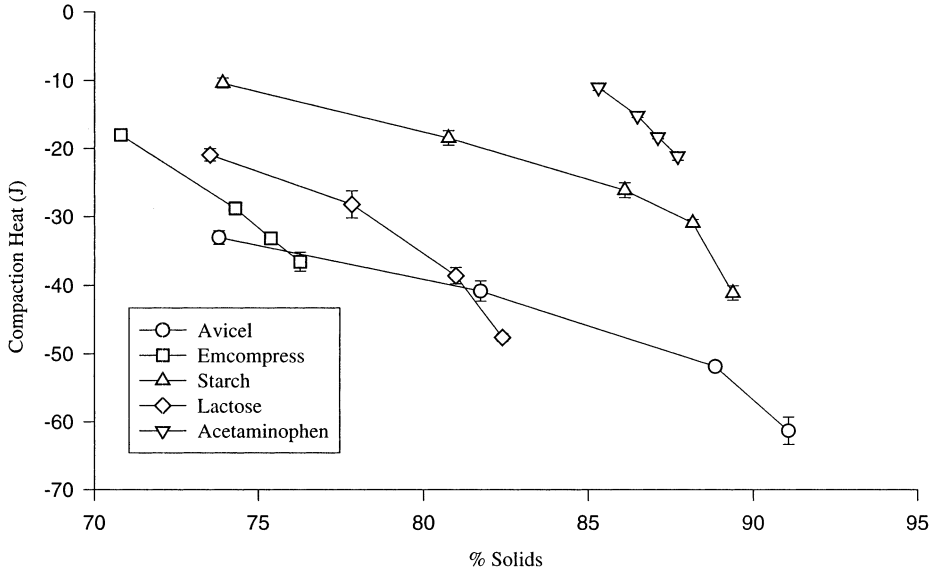

Fig. 11. Compaction heat versus % solids content of compact under load (all points displayed are sample means of $n = 3$ with 2 s error bars).

dynamic property, heat, with respect to compaction force. This investigation also includes heat as a function of percent solids. The formation of a larger number of bonds or stronger bonds yields more heat. Therefore, the data indicate that Avicel® forms more bonds and/or stronger bonds than lactose which forms more bonds than starch. The compaction heat rank order of the materials changes from 15 to 40 kN. This indicates that the rate of bond formation as a function of compaction force, i.e. slope of heat versus force, is different for the materials. Acetaminophen displays the smallest compaction heat which is indicative of its capping nature, as a result of the lack of strong or large number of formed bonds.

Fig. 11 displays compaction heat as a function of % solids content of formed compacts. At 75% solids the rank order from the largest to smallest, with respect to liberated heat, is Avicel®, Emcompress®, lactose, and starch. This indicates that the brittle materials form more bonds and/or stronger bonds than the plastic materials at this percent solids. At 85% solids the rank order is Emcompress® (extrapolated), lactose (extrapolated), Avicel®, and starch. Actual data for Emcompress® and lactose at 85% solids level was unattainable due to the limitation of applied pressures, i.e. force, of the Compaction Simulator. It appears that lactose and Emcompress® yield stronger particle interactions (more bonds and/or stronger bonds) than the plastic materials. Acetaminophen displays the smallest compaction heat as would be expected from the weak and/or lack of sufficient bond formation to form an adherent compact.

3.6. Internal energy change of the compaction process

The change in internal energy of compaction, i.e. compaction energy (ΔE_c), is the net result of the work (W_c) applied and heat (Q_c) liberated during compaction:

$$\Delta E_c = W_c + Q_c \tag{26}$$

The liberated heat of a material is the result of both bond formation and interparticulate friction during consolidation which are confounded. Particle friction is larger for brittle materials which fracture than for plastic materials which flow. Bechard and Down (1992) showed by infrared imaging that localized high-temperature areas were created by interparticulate friction during compaction.

Coffin-Beach and Hollenbeck (1983) reported graphical compression (compaction) energy as a function of compression (compaction) force for Avicel®, lactose, starch, and dicalcium phosphate dihydrate. In contrast to Coffin-Beach's work, Rowlings reported compression (compaction) energy at one compression (compaction) force. In the present investigation, the variability of the compaction energies of the materials, i.e. Fig. 12 (Compaction Energy vs. Maximum Compaction Force), did not allow one to distinguish between the materials at various compaction forces. One difference that is noted is that starch displays a positive change in internal energy below 35 kN. This may be attributed to the loss of bound water from high localized temperature areas. The moisture contents of APAP, Avicel®, Emcompress®, lactose, starch are 0.12, 3.07, 0.75, 0.75, and 8.09%, respectively. As water evaporates, there is a reduction in temperature. However, bond formation causes an increase in temperature. Therefore, for starch, liberated heat is the net result of water evaporation and interparticulate friction and bond formation.

Plotting compaction energy as a function of percent solids (Fig. 13), in contrast to compaction force, differentiates the test materials. At 75% solids, the rank order of negative compaction energy is Emcompress®, Avicel®, and lactose. This may indicate that a brittle material, Emcompress®, forms a larger number of bonds or stronger bonds than does a plastic material, Avicel®, during compaction. Reports have indicated that Avicel® forms stronger/larger number bonds than Emcompress® by evaluation of tensile strength/hardness data. But tensile strength/hardness data are determined from ejected compacts and, therefore, the net result of surviving bonds after compaction, unloading, and ejection.

Emcompress®, appearing to form a larger number of bonds or stronger bonds than Avicel®

under load, yields a larger negative compaction energy. Starch, as discussed previously, displays a positive compaction energy below 89% solids which may be a result of the evaporation of bound moisture. At 85% solids the compaction energy rank order is Emcompress® (extrapolated), lactose (extrapolated), Avicel®, and APAP (extrapolated). This rank order indicates that more/stronger bonds are formed for the brittle materials (Emcompress®, lactose) than for the plastic mate-

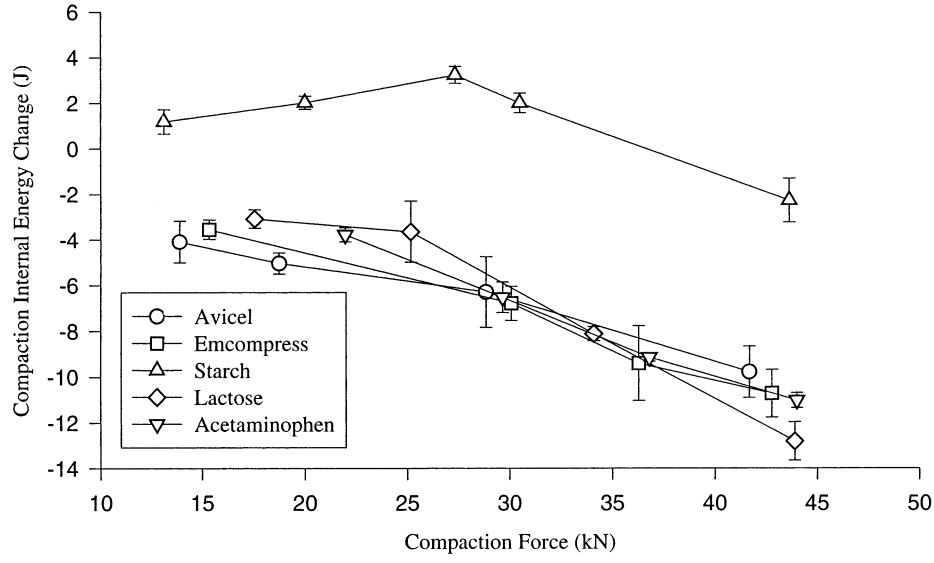

Fig. 12. Compaction internal energy change versus maximum compaction force (all points displayed are sample means of $n = 3$ with 2 s error bars).

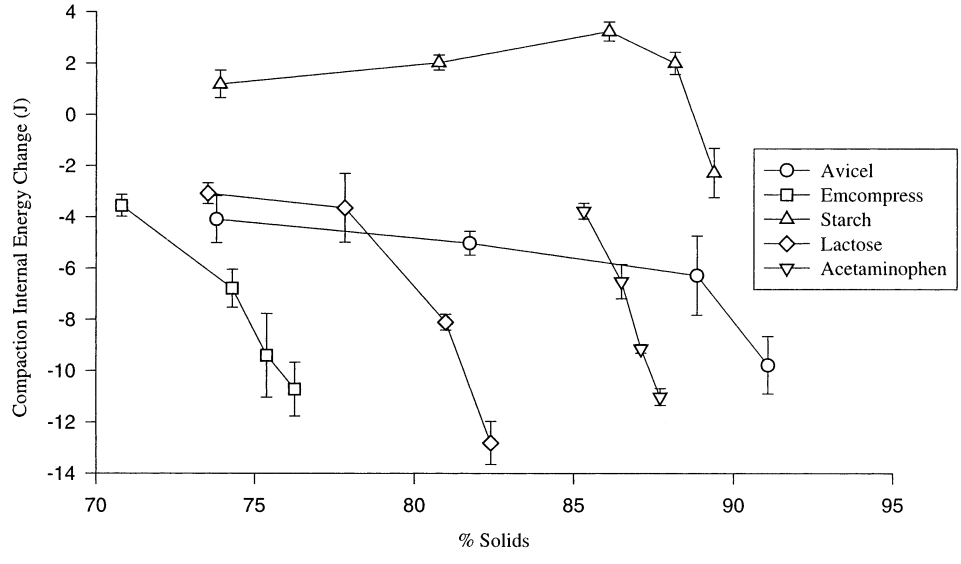

Fig. 13. Compaction energy versus % solids content of compact under load (all points displayed are sample means of $n = 3$ with 2 s error bars).

rial (Avicel®). Again, this bond formation is indicative of the materials under load and not after compact ejection. A future publication will assess the number of surviving bonds after compact ejection which is the net result of compaction, unloading, and ejection.

For all materials, as compaction force increases and, hence, increased solids content, negative compaction energy increases. This is a result of increased particle surface contact which promotes additional bonding. At the largest percent solids level for each material (Fig. 13), it appears that the slopes approach each other. The slopes indicate incremental increase of bond formation as a result of the incremental increase in percent solids from the increase in compaction force.

4. Conclusion

This report describes both the thermal (heat) and mechanical (work) calibration of a 'Compaction Simulator Calorimeter' system. Accurate temperature, force, and displacement measurements provide the means to determine the heat and work of powder compaction, compact unloading, and ejection. The application of a constant strain punch waveform, easily accomplished by a compaction simulator, provides an advantage over other systems by applying a specific/constant quantity of compaction work. Previous investigations used constant stress (force) waveforms which allowed additional compaction work dependent on the creep behavior of the material during compaction. A constant strain waveform assisted in making a more accurate assessment of the thermodynamic process of compaction.

Equations were presented to determine the heat and work values of powder compaction, compact unloading, and compact ejection. Both mechanical energy (work) and thermal energy (heat) calibrations and corrections were reported. Calculation of heat values required the determination of effective and specific heat capacities of the test materials.

A novel graphical technique of reporting compaction work, heat, and energy against percent solids content assisted in evaluating powder compression, consolidation, and bond formation. A plot of compaction energy versus percent solids could differentiate the materials as opposed to a plot of compaction energy versus compaction force. A positive compaction energy was observed for starch below 89% solids (36 kN) which may be a result of bound moisture evaporating from high localized temperature areas of the compact. Avicel®, Emcompress®, lactose, and APAP displayed a negative compaction energy which has been cited as an indication of bond formation (Coffin-Beach, 1982; Coffin-Beach and Hollenbeck, 1983). Brittle materials (Emcompress® and lactose) displayed a larger compaction energy than the plastic materials (Avicel® and starch) and elastic (APAP) materials. This may indicate stronger or larger number of bonds under load for the brittle materials. The evaluation of the subprocess of unloading and ejection are needed in order to make an accurate thermodynamic assessment of the 'tableting' process. This will be reported in subsequent articles.

The evaluation of heat, work, and the change in internal energy, for tablet sub-processes of unloading and ejection of the powder test materials will be reported in subsequent papers.

Acknowledgements

The authors would like to thank SmithKline Beecham Pharmaceuticals for their support of this research. The authors also wish to thank Gary Guy of SmithKline Beecham Pharmaceuticals for his assistance in machining some of the calorimeter parts, and Dr Gary Hollenbeck, University of Maryland, Pharmaceutics Department, for donating the aluminum die and nichrome resistance heater used previously for calorimetry research by David Coffin-Beach (Coffin-Beach, 1982).

References

Bechard, S.R., Down, G.R.B., 1992. Infrared imaging of pharmaceutical materials undergoing compaction. Pharm. Res. 9, 521–528.

Celik, M., 1992. Overview of compaction data analysis techniques. Drug Dev. Ind. Pharm. 18, 767–810.

Celik, M., Maganti, L., 1994. Formulation and compaction of microspheres. Drug Dev. Ind. Pharm. 20, 3151–3173.

Celik, M., Marshall, K., 1989. Use of a compaction simulator system in tabletting research. I. Introduction to and initial experiments with the system. Drug Dev. Ind. Pharm. 15, 759–800.

Celik, M., Okutgen, E., 1993. A feasibility study for the development of a prospective compaction functionality test and the establishment of a compaction data bank. Drug Dev. Ind. Pharm. 19, 2309–2334.

Coffin-Beach, D.P., 1982. A Calorimetric Evaluation of the Compression Process of Several Selected Pharmaceutical Powders, University of Maryland, Dissertation.

Coffin-Beach, D.P., Hollenbeck, R.G., 1983. Determination of the energy of tablet formation during compression of selected pharmaceutical powders. Int. J. Pharm. 17, 313–324.

DeCrosta, M.T., 1998. Thermodynamic Analysis of Compact Formation; Compaction, Unloading, and Ejection, Philadelphia College of Pharmacy and Science, Dissertation.

Dwivedi, S.K., Oates, R.J., Mitchell, A.G., 1992. Estimation of elastic recovery, work of decompression and Young's modulus using a rotary tablet press. J. Pharm. Pharmacol. 44, 459–466.

Esezobo, S., Pilpel, N., 1987. Effects of applied load and particle size on the plastoelasticity and tablet strength of some directly compressible powders. J. Pharm. Pharmacol. 39, 303–304.

Fuhrer, C., Parmentier, W., 1977. Zur thermodynamik der tablettierung. Acta Pharm. Tech. 23, 205–213.

Hanus, E., King, L.D., 1968. Thermodynamic effects in the compression of solids. J. Pharm. Sci. 57, 677–684.

Hiestand, E.N., 1991. Tablet bond. I. A theoretical model. Int. J. Pharm. 67, 217–229.

Higuchi, T., Nelson, E., Busse, L.W., 1954. The physics of tablet compression III. Design and construction of an instrumented tabletting machine. J. Am. Pharm. Assoc. 43, 344–348.

Higuchi, T., Rao, A.N., Busse, L.W., Swintosky, J.V., 1953. The physics of tablet compression. II. The influence of degree of compression on properties of tablets. J. Am. Pharm. Assoc. 42, 194–200.

Hoblitzell, J.R., Rhodes, C.T., 1990. Determination of a relationship between force-displacement and force-time compression curves. Drug. Dev. Ind. Pharm. 16, 201–229.

Holman, L.E., Marshall, K., 1993. Calibration of a compaction simulator for the measurement of tablet thickness during compression. Pharm. Res. 10, 816–822.

Jarvinen, M.J., Juslin, M.J., 1974. On frictional work at the die wall during tablet compression. Farm. Aikak. 83, 1–8.

Jetzer, W., Leuenberger, H., Sucker, H., 1983. Compressibility and compactibility of powder mixtures, November. Pharm. Tech. 33–48.

Juslin, M.J., Jarvinen, M.J., 1971a. Studies on energy expenditure by compressing tablets with an eccentric tablet machine. II. Relationship between mechanical and thermal energy. Farm. Aikak. 80, 297–304.

Juslin, M.J., Krogerus, V.E., 1971b. Studies on tablet lubricants. II. On the effect of some fatty acids, alcohols and hydrocarbons as lubricant judged according to the rise of temperature on the lateral and upper surfaces of the tablets during the tabletting. Farm. Aikak. 80, 197–209.

Ketolainen, J., Ilkka, J., Paronen, P., 1993. Temperature changes during tabletting measured using infrared thermoviewer. Int. J. Pharm. 92, 157–166.

Krogerus, V.E., Kahela, P., Malmivuori, S.I., 1969. An instrumented tablet machine for measuring compressional forces and the rise of temperature of tablets during compression process. Farm. Aikak. 78, 70–78.

Krycer, I., Pope, D.A., Hersey, J.A., 1982. The interpretation of powder compaction data — a critical review. Drug Dev. Ind. Pharm. 8, 307–342.

Lammens, R.F., 1980. The evaluation of force-displacement measurements during one-sided powder compaction in a cylindrical die, University of Leiden, Leiden, Holland, Dissertation.

Lammens, R.F., Liem, T.B., Polderman, J., de Blaey, C.J., 1980b. Evaluation of force-displacement measurements during one-sided powder compaction in a die — the influence of friction with the die wall and of the diameter of punches and die on upper and lower punch pressure. Powd. Tech. 26, 169–185.

Lammens, R.F., Struyk, C., Varkevisser, F.A., Polderman, J., de Blaey, C.J., 1981. Evaluation of force displacement measurements during one-sided powder compaction in a die. The quantitative evaluation of a model of die-wall friction from experiments with various diameters, with a critical examination of the influence of various other machine variables. Powd. Tech. 28, 147–165.

Leuenberger, H., 1982. The compressibility and compactibility of powder systems. Int. J. Pharm. 12, 41–45.

Nelson, E., Busse, L.W., Higuchi, T., 1955. The Physics of tablet compression. VII. Determination of energy expenditure in the tablet compression process. J. Am. Pharm. Assoc. 44, 223–225.

Nurnberg, E., Hopp, A., Temperature measurement during tableting. Pharm. Tech., September, 81–101, 1981.

Oates, R.J., Mitchell, A.G., 1989. Calculation of punch displacement and work of powder compaction on a rotary tablet press. J. Pharm. Pharmacol. 41, 517–523.

Oates, R.J., Mitchell, A.G., 1994. A new method of estimating volume during powder compaction and the work of compaction on a rotary tablet press from measurements of applied vertical force. J. Pharm. Pharmacol. 46, 270–275.

Pesonen, T., Paronen, P., 1990. Compressional behaviour of an agglomerated cellulose powder. Drug Dev. Ind. Pharm. 16, 591–612.

Ragnarsson, G., Sjogren, J., 1983. Work of friction and net work during compaction. J. Pharm. Pharmacol. 35, 201–204.

Ragnarsson, G., Sjogren, J., 1985. Force-displacement measurements in tableting. J. Pharm. Pharmacol. 37, 145–150.

Rankell, A.S., Highuchi, T., 1968. Physics of tablet compression. XV. Thermodynamic and kinetic aspects of adhesion under pressure. J. Pharm. Sci. 57, 574–577.

Rowlings, C.E., 1989. Compression Calorimetry, The University of Iowa, Dissertation.

Rowlings, C.E., Wurster, D.E., Ramsey, P.J., 1995. Calorimetric analysis of powder compression: II. The relationship between energy terms measured with a compression calorimeter and tableting behavior. Int. J. Pharm. 16, 191–200.

Travers, D.N., Merriman, M.P.H., 1970. Temperature changes occurring during the compression and recompression of solids. J. Pharm. Pharmacol. 22:11S–16S.

Travers, D.N., White, J.P., Lewis, C.J., 1972. Thermoelastic properties of preformed compacts. J. Pharm. Pharmacol. 24 Suppl., 57P–66P.

Wadso, I., 1966. Calculation methods in reaction calorimetry. LKB Instrum. J. 13, 33–39.

Wray, P.E., 1992. The physics of tablet compaction revisited. Drug Dev. Ind. Pharm. 18, 627–658.

Wurster, D.E., Creekmore, J.R., 1986. Measurement of the thermal energy evolved upon tablet compression. Drug Dev. Ind. Pharm. 12, 1511–1528.

Wurster, D.E., Rowlings, C.E., Creekmore, J.R., 1995. Calorimetric analysis of powder compression: I. Design and development of a compression calorimeter. Int. J. Pharm. 116, 179–189.

Yu, H.C.M., Rubinstein, M.H., Jackson, I.M., Elsabbagh, H.M., 1988. Multiple compression and plasto-elastic behaviour of paracetamol and microcrystalline cellulose mixtures. J. Pharm. Pharmacol. 40, 669–673.